

R.G. Whittaker, MRCP
J.K. Blackwood, PhD
C.L. Alston, BSc
E.L. Blakely, PhD
J.L. Elson, PhD
R. McFarland, MRCPCH
P.F. Chinnery, FRCP
D.M. Turnbull, FRCP
R.W. Taylor, PhD

URINE HETEROPLASMY IS THE BEST PREDICTOR OF CLINICAL OUTCOME IN THE m.3243A>G mtDNA MUTATION

The m.3243 A>G point mutation in the mitochondrial-encoded *MTTL1* gene is the single most common cause of mitochondrial disease.¹ The range of clinical phenotypes is highly variable, from isolated diabetes and deafness to the devastating mitochondrial encephalomyopathy, lactic acidosis, and stroke-like episodes (MELAS) syndrome.

Mitochondria contain multiple copies of mtDNA, and both wild-type and mutated mtDNA molecules can coexist in the same cell, a condition referred to as heteroplasmy. The expression of different clinical phenotypes is presumed to relate to different heteroplasmy levels within affected tissues.² Being able to predict which patients are likely to develop complications of mitochondrial disease is essential for optimal clinical management. An important question therefore is which of the tissues which are suitable for analysis best reflect the level of mutation in clinically affected tissues, and hence are likely to best predict clinical outcome.

Although the m.3243A>G mutation is readily measurable in blood leukocytes, the level of mutation declines over time.³ Thus even in severely affected patients presenting with MELAS, the level of m.3243A>G mutation may be very low, or even escape detection. Muscle biopsy is the current gold standard for the measurement of heteroplasmy to predict the incidence of specific clinical features. However, although a high heteroplasmy level of the m.3243A>G mutation in muscle increases the probability of developing some of the clinical features seen in this mutation, for example epilepsy and stroke-like episodes, for other clinical features such as myopathy, external ophthalmoplegia, and deafness, this is not the case.⁴ Furthermore, no published data exist as to the stability of mutation load in muscle over time.

In recent years, several laboratories have investigated screening for the m.3243A>G mutation using a range of noninvasive tissues, including hair follicles, fibroblasts, buccal mucosa, and urinary epithelium.^{5,6} Of these, urinary epithelium shows the most consistent mutation load within individual patients. For example, in a small cohort of 12 patients studied over

a 5-year period, we find that there is negligible change in the mutation load of m.3243A>G in urine (J. Blackwood, unpublished data), possibly reflecting replicative differences between urinary epithelium and blood leukocytes, where the mutation is lost. The main advantage of using urine is the ease of obtaining tissue; a 30 mL sample of urine provides enough DNA for accurate detection and quantitation of the m.3243A>G mutation, avoiding the need for patients to undergo a painful and expensive muscle biopsy. We therefore wanted to investigate whether urine was a useful tissue for assessing disease severity.

We studied 24 adult patients harboring the m.3243A>G mutation recruited via a specialist mitochondrial clinic. In all patients, the initial molecular diagnosis had been made using skeletal muscle DNA obtained at muscle biopsy. In addition, an early morning sample of urine and EDTA-blood sample was obtained and the m.3243A>G percentage heteroplasmy level determined. Skeletal muscle and urine samples were obtained from all 24 patients, with blood samples from 21. The time between the initial diagnosis using muscle DNA and subsequent blood and urine samples was 0–6 years. Clinical features were assessed using the Newcastle Mitochondrial Disease Adult Scale (NMDAS), a validated scale in which 29 clinical features are rated according to a numerical scale to give an overall value indicating disease severity.⁷

We examined the correlation between mutation load in these three tissues and disease severity as indicated by the total score on the NMDAS (table). We found a very weak correlation between both blood and muscle m.3243A>G mutation load and total NMDAS score ($\rho = 0.205$, $p = 0.372$ for blood, $\rho = 0.191$, $p = 0.372$ for muscle). The highest correlation with clinical score was with m.3243A>G mutation load in urinary epithelium ($\rho = 0.451$, $p = 0.027$). When we extended the analysis to include all our patients in whom m.3243A>G mutation load in urinary epithelium had been obtained ($n = 58$), we found a similar correlation ($\rho = 0.327$, $p = 0.012$).

Far from being a compromise in terms of ease of obtaining tissue over diagnostic accuracy, screening

Table Comparison of Newcastle Mitochondrial Disease Adult Scale clinical score with m.3243A>G heteroplasmy level in blood, skeletal muscle, and urinary epithelium

Patient ID	Age, y*	Clinical score	Blood heteroplasmy (%)	Muscle heteroplasmy (%)	Urine heteroplasmy (%)
1	33	3	2	4	4
2	45	7	1	11	8
3	78	25	N/A	29	30
4	45	39	16	32	91
5	33	27	14	35	14
6	60	52	6	39	55
7	32	4	1	41	18
8	35	3	8	47	22
9	38	21	8	50	54
10	54	4	14	52	51
11	47	29	2	53	54
12	36	1	14	56	72
13	38	6	16	58	55
14	58	32	24	66	52
15	31	16	16	66	57
16	58	43	N/A	67	60
17	30	1	15	67	62
18	30	50	71	71	96
19	27	5	36	71	52
20	30	32	N/A	71	96
21	63	18	18	76	49
22	41	84	13	81	82
23	50	20	22	87	74
24	29	23	35	87	80

*Refers to the age of the patient at the time that the urine and blood samples were taken and clinical score assessed.

N/A = not available.

of m.3243A>G mutation load in urinary epithelium is a better predictor of outcome than the present gold standard of skeletal muscle tissue. We believe that urinary epithelium completely replaces muscle biopsy as the most suitable tissue for the initial diagnosis in patients suspected of harboring the

m.3243A>G mutation. We have adopted this approach in our practice, and believe that if this approach were to become widespread, then countless patients would avoid the need to undergo an unnecessary muscle biopsy.

From the Mitochondrial Research Group, The Medical School (R.G.W., J.K.B., C.L.A., E.L.B., J.L.E., R.M., P.F.C., D.M.T., R.W.T.), and Institutes of Human Genetics and Ageing and Health (P.F.C., D.M.T., R.W.T.), Newcastle University, Newcastle upon Tyne, UK.

Funded by a project grant from SPARKS and by the Wellcome Trust. R.G.W. is funded by EUmitocombat.

Disclosure: The authors report no disclosures.

Received August 12, 2008. Accepted in final form September 15, 2008.

Address correspondence and reprint requests to Dr. Roger G. Whittaker, Mitochondrial Research Group, The Medical School, Newcastle University, Framlington Place, Newcastle upon Tyne, NE2 4HH, UK; r.whittaker@ncl.ac.uk

Copyright © 2009 by AAN Enterprises, Inc.

1. Schaefer AM, McFarland R, Blakely EL, et al. Prevalence of mitochondrial DNA disease in adults. *Ann Neurol* 2008;63:35–39.
2. Macmillan C, Lach B, Shoubridge EA. Variable distribution of mutant mitochondrial DNAs (tRNA(Leu[3243])) in tissues of symptomatic relatives with MELAS: the role of mitotic segregation. *Neurology* 1993;43:1586–1590.
3. Rahman S, Poulton J, Marchington D, et al. Decrease of 3243 A>G mtDNA mutation from blood in MELAS syndrome: a longitudinal study. *Am J Hum Genet* 2001;68:238–240.
4. Chinnery PF, Howell N, Lightowlers RN, et al. Molecular pathology of MELAS and MERRF. The relationship between mutation load and clinical phenotypes. *Brain* 1997;120:1713–1721.
5. Shanske S, Pancrudo J, Kaufmann P, et al. Varying loads of the mitochondrial DNA A3243G mutation in different tissues: implications for diagnosis. *Am J Med Genet A* 2004;130A:134–137.
6. McDonnell MT, Schaefer AM, Blakely EL, et al. Noninvasive diagnosis of the 3243A>G mitochondrial DNA mutation using urinary epithelial cells. *Eur J Hum Genet* 2004;12:778–781.
7. Schaefer AM, Phoenix C, Elson JL, et al. Mitochondrial disease in adults: a scale to monitor progression and treatment. *Neurology* 2006;66:1932–1934.

A.L. Green, FRCS(SN)
S. Wang, PhD
J.F. Stein, D Phil
E.A.C. Pereira, MB ChB
M.L. Kringelbach, D Phil
X. Liu, PhD
J.-S. Brittain, PhD
T.Z. Aziz, D Med Sci

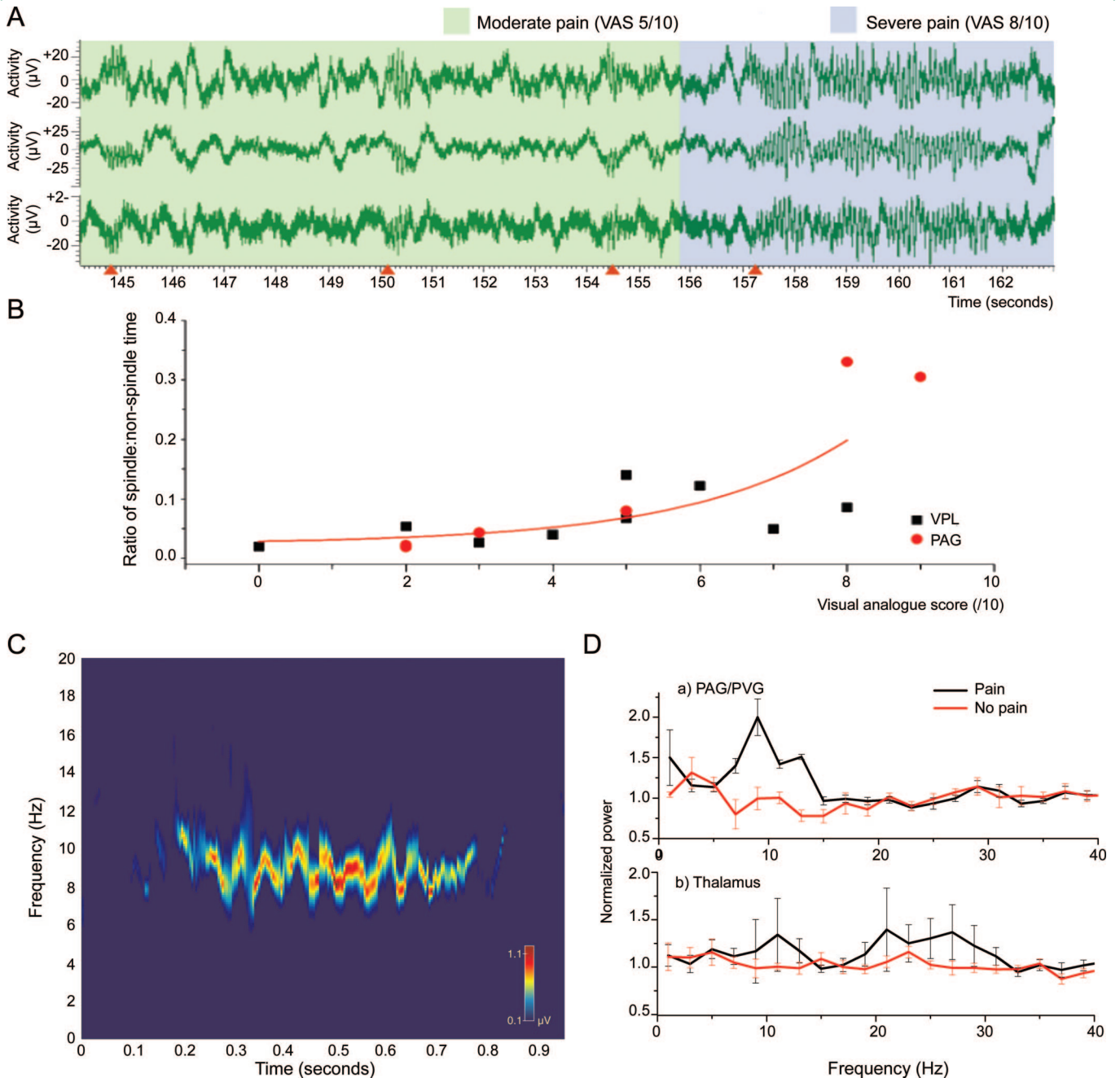
NEURAL SIGNATURES IN PATIENTS WITH NEUROPATHIC PAIN

The mechanisms by which neural signals are encoded to produce conscious sensations remain a central question in neuroscience. Invasive recordings from human brain structures in vivo give us the opportunity to study neural correlates of these sensations. Pain is a sensation fundamental to survival and its subjective nature in the clinical setting makes it difficult to quantify. It remains without direct objective neuronal correlates. Here we describe an 8–14 Hz,

spindle-shaped neural signal present in both the sensory thalamus and periaqueductal gray area (PAG) in humans that directly correlates to the subjective reporting of pain intensity.

Local field potentials (LFPs) recorded by deep brain macroelectrodes reveal the ensemble activity of neuronal groups in particular brain regions.¹ The oscillatory amplitude of such ensembles is proportionate to the degree of synchrony with which they oscillate.² Properties of oscillations including their synchrony, frequency, and corre-

Figure Local field potential changes in different pain states



(A) 10-Hz spindle-shaped activity in the ventroposterolateral nucleus of the thalamus in a patient with chronic neuropathic poststroke pain. The three graphs represent three bipolar channels of the same electrode (four contacts). Note the onset of each period of activity as indicated by the orange arrows on the x-axis as well as the relative pain that the patient was experiencing, as indicated by the colored overlay (green = moderate pain [VAS = 5/10], blue = severe pain [VAS = 9/10]). (B) Comparison of spindle–nonspindle activity in each nucleus showed a significant exponential correlation between VAS and spindle activity. Each point represents a different patient (15 electrodes in 12 patients, as 3 had PAG and VPL). $R^2 = 0.67$, $\chi^2 = 0.00373$. (C) Time-frequency analysis of local field potentials during pain. This shows a 1-second segment of the power spectrum of the local field potentials recorded from the sensory thalamus in a patient with intense pain (VAS = 8/10). Based on time-variant autoregressive modeling, this time-frequency distribution demonstrates the changes in dominant frequencies during a 1-second burst of spindle activity over time. It demonstrates the maximum power of approximately 8–10 Hz with entry from high frequency to low frequency during the 1-second burst of spindle activity. This provides an individual signature of pain for this patient. Frequencies above 20 Hz have been omitted for clarity. (D) Mean power spectral changes for each nucleus. Power spectra showing the dominant frequencies for each nucleus in two conditions. In the nonpain condition, patients were at rest. In the painful condition, pain was evoked using an ice-cold stimulus on the skin of the affected part. Pain increases power in the 8–12 Hz frequency in the PAG and 17–30 Hz in the sensory thalamus. Light-colored lines show 1 SD of the mean. VAS = Visual Analogue Score; PVG = periventricular gray area; PAG = periaqueductal gray area; VPL = ventroposterolateral.

sponding power spectra vary both between brain structures and dynamically, depending upon the activity performed.³

Methods. Twelve patients (11 male, 1 female) underwent deep brain stimulation for treatment of chronic neuropathic pain. Etiology was as follows; poststroke pain (4), phantom limb pain (3), facial pain of various causes (4), and brachial plexus injury (1). Nuclei targeted were periaqueductal gray (PAG) alone in 3 patients, ventroposterolateral/medial nucleus of the thalamus (VPL/VPM) in 6 patients, and both in 3 patients. This was decided upon based on clinical grounds (in general, sensory thalamus was avoided if the patient had had a thalamic stroke). Three patients had both nuclei implanted as stimulation of the first did not show convincing pain relief intraoperatively. Mean age was 51.6 years (range 35–74 years).

LFPs were recorded postoperatively. The experiment was started with 10 minutes of rest before recording. Recording of LFPs then lasted 10 minutes, during which time Visual Analogue Score (VAS) of pain was recorded every 60 seconds. This protocol was repeated three times for each patient, on 3 separate days.

Results. The most prominent finding was characteristic spindle-shaped bursts of increased amplitude at approximately 10 Hz (slightly different in different subjects, range 8–14 Hz, mean 10 Hz) in both the sensory thalamus and PAG concomitant with subjective awareness of pain (figure, A). Statistical analysis revealed a significant increase in the number of bursts and increasing VAS for each individual subject as well as an increased ratio of burst-time to non-burst-time activity in the pain state (figure, B). Plotting burst activity against the background power spectrum of LFP activity over a finite time course reveals an individual neural signature of pain for each subject (figure, C). In general, power spectra reveal that there is a significant rise in the 8–12 Hz activity in the PAG and a rise in the 17–30 Hz activity, i.e., beta frequency, in the sensory thalamus (figure, D).

Discussion. Noninvasive electrophysiologic and functional neuroimaging technologies have, until now, provided the most convincing evidence of changes in human brain activity associated with pain.⁴ They have also enhanced understanding of whole brain responses to deep brain stimulation.⁵ Although previous studies have looked at electrical coupling between brain nuclei in pain,⁶ they have not revealed convincing characteristic waveforms that may represent pain perception. These previous stud-

ies have suggested 0.2–0.4 Hz frequency changes in the sensory thalamus in the pain state, but these frequencies were reduced during analgesia induced by periventricular gray area stimulation and this frequency is rather close to that of respiration. The correlation of the pain spindles in the thalamus may be explained by the fact that they represent direct activity in a relay nucleus. In the PAG, they are harder to understand as this is an antinociceptive area but they may be due to the “pain inhibits pain” mechanism of diffuse noxious inhibitory controls on which the PAG has been shown to have an influence.⁷ Our findings are significant in that not only do they provide a direct neural signature of a subjective conscious state but they may also allow for objective measurements and predictions of the relative level of subjective pain. We intend to investigate these preliminary findings in a more methodical and robust manner.

From the Department of Physiology, Anatomy & Genetics (A.L.G., S.W., J.F.S., E.A.C.P., M.L.K., T.Z.A.), University of Oxford; Department of Neurosurgery (A.L.G., J.-S.B., T.Z.A.), West Wing, John Radcliffe Hospital, Oxford; and Division of Neurosciences & Mental Health (X.L.), Imperial College London, Charing Cross Campus, London, UK.

Shouyan Wang is supported by the Norman Collison Foundation, and Tipu Aziz by the Medical Research Council, Wellcome Trust, and Templeton Foundation.

Disclosure: The authors report no disclosures.

Received July 16, 2008. Accepted in final form September 16, 2008.

Address correspondence and reprint requests to Dr. Alexander L. Green, Department of Neurosurgery, West Wing Level 3, John Radcliffe Hospital, Oxford, OX3 9DU, UK; alex.green@nds.ox.ac.uk

Copyright © 2009 by AAN Enterprises, Inc.

AUTHOR CONTRIBUTIONS

The statistical analysis was performed by A.L.G.

1. Buzsaki G. Large-scale recording of neuronal ensembles. *Nat Neurosci* 2004;7:446–451.
2. Pfurtscheller G, Lopes da Silva FH. Event-related EEG/MEG synchronization and desynchronization: basic principles. *Clin Neurophysiol* 1999;110:1842–1857.
3. Engel AK, Fries P, Singer W. Dynamic predictions: oscillations and synchrony in top-down processing. *Nat Rev Neurosci* 2001;2:704–716.
4. Peyron R, Laurent B, Garcia-Larrea L. Functional imaging of brain responses to pain. A review and meta-analysis. *Neurophysiol Clin* 2000;30:263–288.
5. Kringelbach ML, Jenkinson N, Green AL, et al. Deep brain stimulation for chronic pain investigated with magnetoencephalography. *Neuroreport* 2007;18:223–228.
6. Nandi D, Aziz T, Carter H, et al. Thalamic field potentials in chronic central pain treated by periventricular gray stimulation: a series of eight cases. *Pain* 2003;101:97–107.
7. Bouhassira D, Villanueva L, Le Bars D. Effects of systemic morphine on diffuse noxious inhibitory controls: role of the periaqueductal grey. *Eur J Pharmacol* 1992;216:149–156.

OCULAR TILT REACTION: A CLINICAL SIGN OF CEREBELLAR INFARCTIONS?



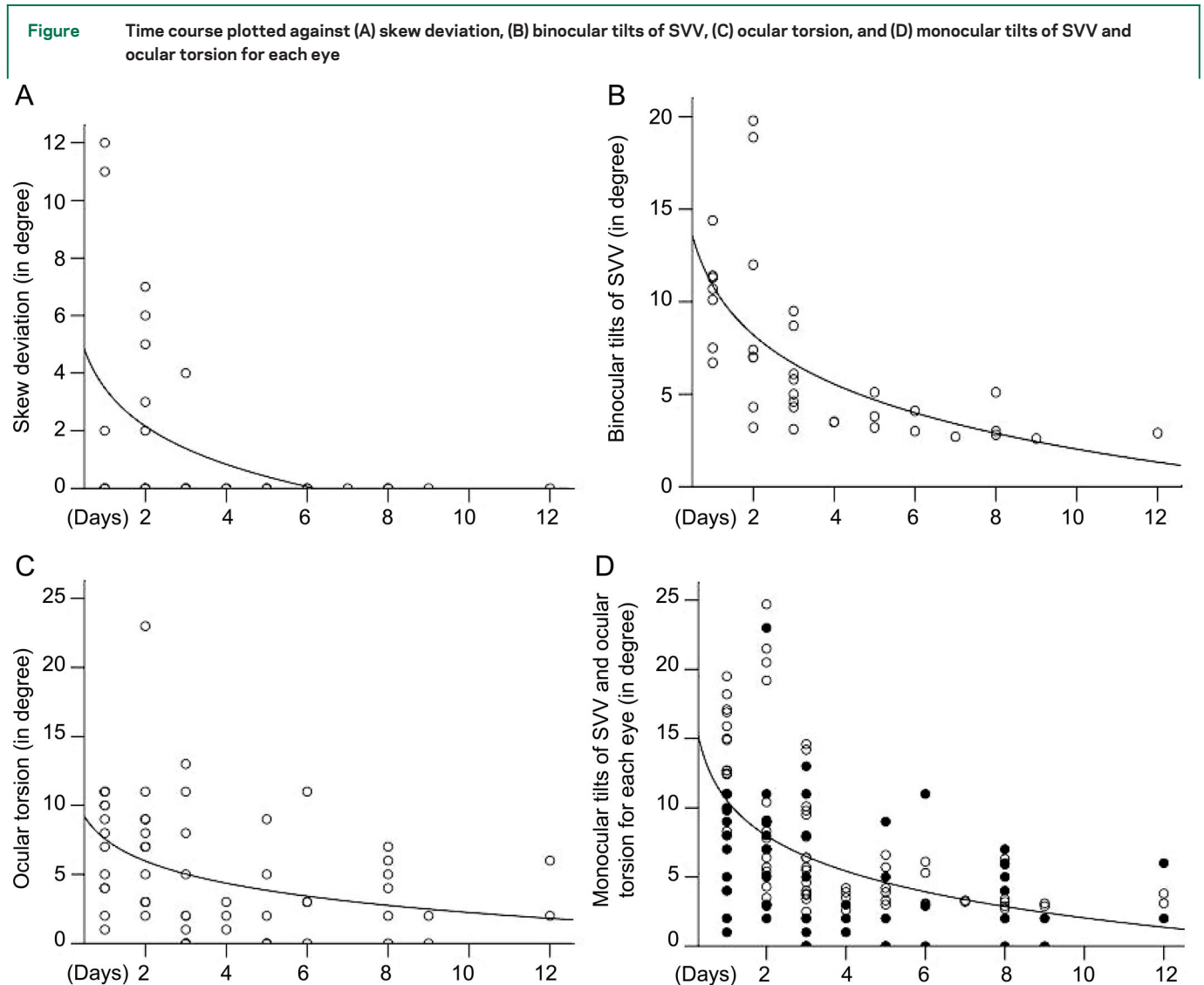
Ocular tilt reaction (OTR) consists of head tilt, ocular torsion (OT), and skew deviation (SKD) combined with perceptual tilts such as deviations of the subjective visual vertical (SVV). Few case reports have shown that OTR also occurs in patients with cerebellar infarctions.¹⁻⁴ However, no systematic clinical studies are available on the frequency of signs of OTR in patients with cerebellar lesions. Therefore, the questions arose as to whether OTR is a common clinical sign of an acute cerebellar lesion and whether the time course of its components is similar to those from brainstem infarctions. The cerebellar structures involved in 31 patients were studied in detail elsewhere.⁵

Supplemental data at www.neurology.org

Methods. All 56 patients with acute unilateral cerebellar infarctions (51 ischemic; 5 hemorrhagic) admitted at

our department were included in the study (median age 65 years, range 37–84 years; 37 men and 19 women). Forty-three patients had unilateral, and 13 patients with unilateral cerebellar infarctions had additional brainstem lesions (27 patients had right-sided, 29 left-sided lesions). All patients underwent a neuro-ophthalmologic examination including testing tilt of SVV, OT, SKD (for details, see the video⁵), electronystagmography including caloric irrigation, and MRI scanning. Only two of the patients with infarctions in the territory of the anterior inferior cerebellar artery showed a unilateral hypo-responsiveness in the caloric testing. The median latency between infarction and investigation was 3 days (range 1–12 days). The vascular territory was determined by using the anatomic diagrams of Tatu et al.⁶

Results. Most of the 43 patients with purely unilateral cerebellar lesions presented with contralateral



Open circles represent monocular tilts of subjective visual vertical (SVV) of each eye; filled circles represent ocular torsion of each eye. Only absolute values were taken.

signs: 58% showed tilts of SVV (median of the binocular SVV deviation 5.1°), whereas 35% had OT (median net tilt angle of OT of the right eyes: 7°; and of the left eyes: 5°) and 14% SKD (median 3°). Ipsilateral signs were less frequent: 26% had tilts of SVV (median SVV deviation 5.8°), 14% OT, and 9% SKD (median net tilt angle of the right eyes: 6°; and of SKD 5°). For both ipsi- and contralateral signs of OTR, all patients with SKD (9 patients) also showed the other signs of OTR. Thus, a complete OTR was seen in 21% (table e-1 on the *Neurology*® Web site at www.neurology.org).

The patients with combined cerebellar and brainstem lesions showed opposite results: only 15% (2 patients) had contralateral (SVV deviation 7.0° and 3.0°), but 46% had ipsilateral tilts of SVV (median 5.0°). Contralateral OT occurred in 15% (2 patients) (net tilt angle of the right eyes: 5°, 11°; and of the left eyes: 7°, 13°) and ipsilateral OT in 23% of the patients (median net tilt angle of the right eyes: 7.5°, and of the left eyes: 6°). Contralateral SKD was seen in one patient (5°); none had an ipsilateral SKD. Thus, there was a difference of the frequency between contra- and ipsilateral tilts of SVV in patients with pure and combined cerebellar lesions ($\chi^2 19.58$; $p = 0$). This indicates that more patients with purely cerebellar lesions had contralateral tilts of SVV.

In patients with pure unilateral cerebellar lesions, the nonlinear regression models ($p < 0.01$) suggest that with increasing time since lesion, OT and tilts of the SVV last longer than 10 days, whereas SKD wears off within around 6 days (figure).

Discussion. Our data give evidence that OTR is a common sign in patients with unilateral cerebellar lesions, indicating that lesions of the cerebellum induce a dysfunction in otoliths pathways that mediate vestibular information in the roll plane.

Single components such as tilts of the SVV can occur in up to 85% and show similar time courses to those in brainstem infarctions⁷ with the skew deviation as the most transient sign. However, the amount of the deviations in the acute phase was less in patients with cerebellar lesions (median of contralateral [5.1°] and ipsilateral SVV deviation [5.8°]), and highest in patients with medullary brainstem infarctions (Wallenberg syndrome, 9.8°) compared to that in acute vestibular neuritis (7.0°).⁷

Thus, signs of OTR not only indicate brainstem, thalamic, or peripheral vestibular lesions but also unilateral cerebellar lesions, which affect structures involved in the processing of vestibular signals. These structures seem to form a pathway from the brainstem to the vermis (including the cerebellar peduncles, the dentate nucleus, pyramid of the vermis, nodulus, and uvula) and to the flocculus and tonsil.⁵

The specific structures lesioned, however, determine the directive of the signs, ipsilateral or contralateral. An affection of the dentate nucleus in particular was associated with contralateral signs of OTR, whereas in ipsilateral signs the dentate nucleus was spared and lesions were located in the middle cerebellar peduncle, tonsil, biventer, and inferior semilunar lobules.⁵

From the Department of Neurology (B.B., M.D.), University of Mainz; and Department of Neurology (M.D.), Ludwig-Maximilians-University, Munich, Germany.

Supported by the DFG (DI 379/4-4).

Disclosure: The authors report no disclosures.

Received April 29, 2008. Accepted in final form September 24, 2008.

Address correspondence and reprint requests to Dr. Bernhard Baier, Department of Neurology, University of Mainz, Langenbeckstr. 1, 55131 Mainz, Germany; baierb@uni-mainz.de

Copyright © 2009 by AAN Enterprises, Inc.

AUTHOR CONTRIBUTIONS

The statistical analysis was conducted by B.B.

ACKNOWLEDGMENT

The authors thank Mrs. Benson for critically reading the manuscript.

1. Mossman S, Halmagyi GM. Partial ocular tilt reaction due to unilateral cerebellar lesion. *Neurology* 1997;49:491–493.
2. Min W, Kim J, Park S, Suh C. Ocular tilt reaction due to unilateral cerebellar lesion. *Neuroophthalmology* 1999;22:81–85.
3. Lee H, Lee SY, Lee SR, Park BR, Baloh RW. Ocular tilt reaction and anterior inferior cerebellar artery syndrome. *J Neurol Neurosurg Psychiatry* 2005;76:1742–1743.
4. Wong AM, Sharpe JA. Cerebellar skew deviation and the torsional vestibuloocular reflex. *Neurology* 2005;65:412–419.
5. Baier B, Bense S, Dieterich M. Are signs of ocular tilt reaction in patients with cerebellar lesions mediated by the dentate nucleus? *Brain* 2008;131:1445–1454.
6. Tatu L, Moulin T, Bogousslavsky J, Duvernoy H. Arterial territories of human brain. *Brainstem and cerebellum*. *Neurology* 1996;47:1125–1135.
7. Cnyrim CD, Rettinger M, Mansmann U, et al. Central compensation of deviated subjective visual vertical in Wallenberg's syndrome. *J Neurol Neurosurg Psychiatry* 2007;78:527–528.